

Oxygen Concentration Determines Regiospecificity in Soybean Lipoxygenase-1 Reaction Via a Branched Kinetic Scheme*

(Received for publication, August 1, 1997)

Hugues Berry‡, H el ene D ebat‡, and V eronique Larreta Garde§¶

From the ‡Laboratory of Enzyme Technology, UPRES A 6022 CNRS, University of Compi egne, B.P. 20.529, 60205 Compi egne, France and §Ermece, Department of Life Sciences, University of Cergy-Pontoise, 2, avenue Adolphe Chauvin, 95302 Cergy-Pontoise Cedex, France

The effect of oxygen concentration on the regiospecificity of the soybean lipoxygenase-1 dioxygenation reaction was studied. At low oxygen concentrations (<5 μM), a dramatic change in the regiospecificity of the enzyme was observed with the hydroperoxy-octadecadienoic acid (HPOD) 13:9 ratio closer to 50:50 instead of the generally reported 95:5. This alteration of regiospecificity is not an isolated phenomenon, since it occurs during a reaction carried out under "classical" conditions, *i.e.* in a buffer saturated with air before the reaction. β -carotene bleaching and electronic paramagnetic resonance findings provided evidence that substrate-derived free radical species are released from the enzyme. The kinetic scheme proposed by Schilstra *et al.* (Schilstra, M. J., Veldink, G. A. & Vliegthart, J. F. G. (1994) *Biochemistry* 33, 3974–3979) was thus expanded to account for the observed variations in specificity. The equations describing the branched scheme show two different kinetic pathways: a fully enzymatic one leading to a regioisomeric composition of 13-HPOD:9-HPOD = 95:5, and a semienzymatic one leading to a regioisomeric composition of 13-HPOD:9-HPOD = 50:50. The ratio between the two different pathways depends on oxygen concentration, which thus determines the overall specificity of the reaction.

Lipoxygenases (EC 1.13.11.12) are widely distributed in both the animal and plant kingdoms. They catalyze the dioxygenation of unsaturated fatty acids containing one or more (1Z,4Z)-pentadiene systems into the corresponding conjugated hydroperoxides. In animal tissues, the most frequently encountered substrate is arachidonic acid ($\text{C}_{20:4}$), which is dioxygenated by lipoxygenases into precursors of products involved in inflammatory processes (2), cell membrane maturation (3), or cancer metastasis (4). The role of plant lipoxygenases, whose main substrates are linoleic ($\text{C}_{18:2}$) and linolenic ($\text{C}_{18:3}$) acids, is not yet fully elucidated, although they are implied in processes such as senescence or plant response to wounding (5).

A single non-heme iron is present in each enzyme and can exist in two oxidation states: Fe(II) and Fe(III) (6). According to the current working mechanism (1, 6, 7), the native enzyme, as obtained when purified, is inactive and in the Fe(II) form. When treated with an equimolar amount of product, the iron is oxidized to the Fe(III) form, resulting in an active enzyme. This

ferric form can then catalyze the abstraction of a hydrogen from the bis-allylic carbon atom of the substrate (S) in a stereospecific manner, yielding a pentadienyl radical (S') complexed with the ferrous enzyme. Bimolecular oxygen is then added to the pentadienyl radical, either at the C-1 or the C-5 of the pentadiene system, which leads to the formation of the hydroperoxide product (P) and the reoxidation of the cofactor to the ferric form (see Scheme 1, *upper part*).

This cycling between the ferric and ferrous forms thus plays a crucial role in catalysis. The existence of product activation of the enzyme explains the lag time observed in kinetics occurring under certain conditions, especially with a high initial [Substrate]/[Product] ratio (1). During the reaction, a small fraction of the complex formed by the ferrous enzyme and the pentadienyl radical can also dissociate, regenerating the inactive ferrous enzyme form. A steady-state level of Fe(II) enzyme is gradually approached.

Moreover, the position at which dioxygen is inserted defines the regiospecificity of the enzyme. Under most conditions, soybean lipoxygenase-1 is highly specific for the insertion of dioxygen on the C-13 atom of linoleic acid (yielding 13-HPOD¹) or on the C-15 atom of arachidonic acid yielding 15-hydroperoxyeicosatetraenoic acid (10, 11). However, this marked specificity can be modulated by certain factors especially pH (12, 13) or substrate structure in the reaction medium (14, 15). Almost every attempt to explain the observed variations in specificity has been based on modifications of the substrate (charge of the carboxylate group, for example) or of the enzyme. A kinetic model in which the position of dioxygen insertion proceeds through two different enzymatic pathways, the overall specificity being a function of the $K_{M(\text{O}_2)}$ for each of the two pathways, has been proposed (16). Nevertheless, this model fails to explain the specificity modifications observed with varying pH.

In the present study, we tried to determine and explain the influence of oxygen concentration on soybean lipoxygenase-1 specificity, in keeping with the current kinetic model. The oxygen concentration in a reaction medium at any given time is a function of two parameters: the initial oxygen concentration and the rate of oxygen consumption by the reaction itself. Thus we varied initial and continuous oxygenation conditions (N_2 , O_2 or air bubbling). We also used sorbitol, a polyol which acts as soluble cosolvent. In previous studies, we have shown that such

* The costs of publication of this article were defrayed in part by the payment of page charges. This article must therefore be hereby marked "advertisement" in accordance with 18 U.S.C. Section 1734 solely to indicate this fact.

¶ To whom correspondence should be addressed. Tel.: 33-1-34-25-66-05; Fax: 33-1-34-25-65-20; E-mail: larreta@u-cergy.fr.

¹ The abbreviations used are: HPOD, hydroperoxyoctadecadienoic acid; 13:9 ratio, ratio between the two regio-isomer products 13-HPOD and 9-HPOD, calculated with 9-HPOD(%) = $[9\text{-HPOD}] \times 100 / ([13\text{-HPOD}] + [9\text{-HPOD}])$; LA, linoleic acid; OC, oxygen consumption phase; SP, pseudo-stationary phase; DP, headspace oxygen dissolution phase; P, fully enzymatically formed hydroperoxide product; Q, semienzymatically formed hydroperoxide product; S', pentadienyl radical; $\text{SO}_2^{\cdot-}$, peroxy radical; k_1 , k_2 , k_4 , monomolecular rate constants; k_3 , k_5 , k_6 , k_7 , bimolecular rate constants; K_{mS} , K_{iS} , K_{mP} , K_{iP} , equilibrium (dissociation) constants.

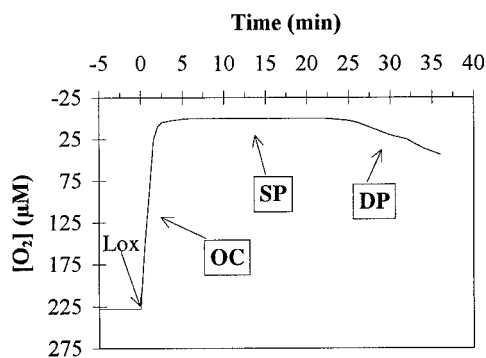


FIG. 1. Typical course of a dioxygenation reaction initiated by soybean lipoxygenase-1 (LOX), under oxygen concentrations limiting relative to substrate as followed by a Clark electrode. $[LA] = 400 \mu\text{M}$. The three phases are OC, SP, and DP.

TABLE I

Soybean lipoxygenase-1 specificity with air (panels A and B, $[O_2]_{\text{initial}} = 228 \mu\text{M}$) or oxygen (panel C, $[O_2]_{\text{initial}} = 1140 \mu\text{M}$) bubbling before the beginning of the reaction

Panel A, $[LA]_{\text{initial}} = 300 \mu\text{M}$; panel B, $[LA]_{\text{initial}} = 190 \mu\text{M}$; panel C, $[LA]_{\text{initial}} = 800 \mu\text{M}$. The column labeled "Reaction phase" refers to the reaction phase at the end of which the 13:9 ratio has been determined.

	$[O_2]$	$[LA]$	[Sorbitol]	Reaction phase	13:9 Ratio
	μM	μM	M		
Panel A	228	300	0	OC	95:5
			0	SP	89:11
			2	OC	94:6
			2	SP	82:18
Panel B	228	190	2	SP	95:5
Panel C	1140	800	0	OC	95:5
			0	SP	95:5
			2	OC	95:5
			2	SP	96:4

strate concentrations (i.e. $[O_2]_{\text{initial}} > [S]_{\text{initial}}$), this specificity variation is not observed (Table I, panels B and C). Under these conditions, specificity is independent of the reaction phase or the presence of sorbitol. Fig. 2 shows that the higher the $[S]/[O_2]$ ratio, the greater the change in specificity toward 9-HPOD formation at the end of the SP; under high oxygen concentrations (continuous oxygen bubbling throughout the reaction), the specificity is not altered (Fig. 2, \square). Moreover, the specificity varies with substrate concentration; the 9-HPOD percentage increases with increasing linoleic acid concentrations (Fig. 2).

Incubation of a 13-HPOD:9-HPOD mixture in an initial 95:5 ratio, without substrate and with or without enzyme, does not change the isomeric composition of the product (data not shown). Thus the regiospecificity modification is not caused by an enzyme-dependent or -independent isomerization of the product. Neither can it be due to linoleic acid autoxidation, since a 2-h incubation of buffer containing substrate but no enzyme failed to give rise to HPOD amounts comparable to those observed here (data not shown).

Hence, the observed variation of specificity occurs when oxygen concentration is limiting relative to substrate. Assuming a stoichiometry of 1:1 during the OC phase between oxygen and substrate enzymatic consumption, some untransformed substrate remains at the beginning of the SP when $[O_2]_{\text{initial}} < [S]_{\text{initial}}$. Thus, the specificity variation is related to the presence of residual substrate at the beginning of the second phase (SP).

Furthermore, when N_2 is flushed in the reactor headspace at

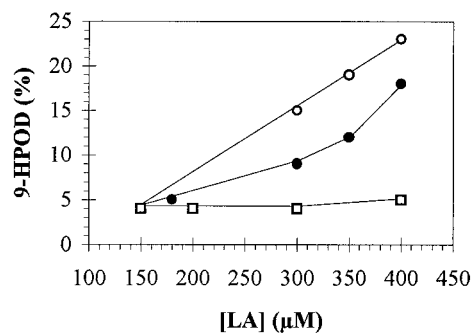


FIG. 2. Regiospecificity of the dioxygenation reaction at the end of the pseudo-stationary phase (SP) without bubbling (\circ) or with continuous bubbling of the buffer throughout the reaction with either air (\bullet) or oxygen (\square). 9-HPOD(%) refers to 9-HPOD percentage relative to $([13\text{-HPOD}] + [9\text{-HPOD}])$.

the beginning of SP, this specificity variation is not observed (Fig. 3). This implies that the specificity alteration occurs when the conditions are not completely anaerobic during SP. During this phase, the apparent oxygen concentration represents the difference between the oxygen dissolution rate and the enzyme activity rate. As shown in Table II, except for pure oxygen bubbling in buffer, oxygen dissolution from the reactor headspace into the buffer is always slower than its consumption by the reaction, resulting in apparently null oxygen concentrations (Fig. 1). This implies that the oxygen concentration during the SP allows some dioxygenation to occur. In fact, oxygen concentration during the SP is actually stationary as the enzymatic reaction is not really over before the beginning of the DP. For this reason, the duration of the SP increases with substrate concentration (data not shown).

Table II also shows that oxygen dissolution rates are approximately 10 times lower when 2 M sorbitol is added to the buffer. As the enzymatic reaction rate with added sorbitol is higher (17), the available oxygen concentration during the pseudo-stationary phase is decreased in the presence of this polyol. This would account for the greater specificity variation at the end of SP, when 2 M sorbitol is added in the buffer.

Lipoxygenase Specificity at Low Oxygen Concentrations—When the reaction buffer is bubbled with N_2 before the reaction (i.e. $[O_2]_{\text{initial}} < 5 \mu\text{M}$), soybean lipoxygenase-1 catalyzes the oxygenation reaction with a specificity dramatically different from that observed with higher oxygen concentrations (Fig. 4); the enzyme produces almost equal amounts of 13- and 9-HPOD throughout the reaction course (13:9 ratio $\approx 55:45$). This ratio is similar to that observed in the auto-oxidation reaction (24).

Assuming that all the substrate has been transformed at the beginning of the headspace oxygen dissolution phase (DP) and that the substrate is transformed during the first phase (OC) with a 13:9 ratio = 95:5, the specificity occurring during the SP phase of a reaction initiated at oxygen concentrations limiting relative to substrate, has been estimated at

$$\frac{(\%9\text{-HPOD})_{\text{SP}}}{100} = \left\{ \frac{([S]_i \times ((\%9\text{-HPOD})_{\text{DP}}/100)) - ([O_2]_i \times 0.05)}{[S]_i - [O_2]_i} \right\} \quad (\text{Eq. 1a})$$

where $(\%9\text{-HPOD})_{\text{SP}}$ is the calculated 9-HPOD percentage relative to $([13\text{-HPOD}] + [9\text{-HPOD}])$ occurring during the pseudo-stationary phase SP; $[S]_i$ is the initial linoleic acid concentration; $(\%9\text{-HPOD})_{\text{DP}}$ is the 9-HPOD percentage relative to $([13\text{-HPOD}] + [9\text{-HPOD}])$ observed at the beginning of the headspace oxygen dissolution phase DP (end of the reaction) $[O_2]_i$ is the initial oxygen concentration.

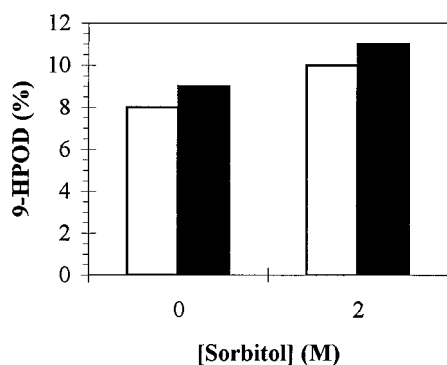


FIG. 3. Regiospecificity of the dioxygenation reaction at the end of the oxygen consumption phase OC (□) or at the end of the stationary phase SP with N_2 flushing the reactor headspace at the beginning of SP (■). $[LA]_{\text{initial}} = 300 \mu\text{M}$; $[O_2]_{\text{initial}} = 230 \mu\text{M}$.

TABLE II
Initial rates of oxygen dissolution and enzyme reaction in air- or oxygen-saturated buffer with or without 2 M sorbitol as determined by pO_2 measurements (Clark electrode)

	Pure O_2 bubbling		Air bubbling	
	Enzyme reaction rate	Oxygen dissolution rate	Enzyme reaction rate	Oxygen dissolution rate
		$\mu\text{M min}^{-1}$		
0.1 M Pyrophosphate buffer	235	705	141	130
0.1 M Pyrophosphate buffer + 2 M sorbitol	280	77	165	14

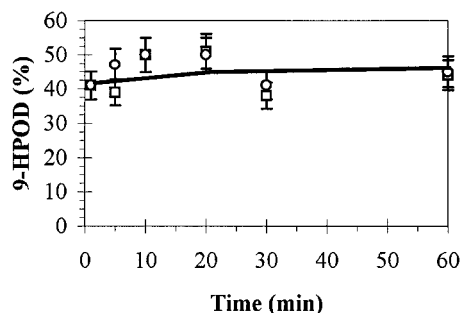


FIG. 4. Regiospecificity of the dioxygenation reaction initiated at low initial oxygen concentration (initial N_2 bubbling) in buffer (□) or 2 M sorbitol containing buffer (○). $[LA]_{\text{initial}} = 300 \mu\text{M}$; $[O_2]_{\text{initial}} < 5 \mu\text{M}$.

Fig. 5 shows that the calculated $(\%9\text{-HPOD})_{\text{SP}}$, *i.e.* the calculated specificity occurring during the SP phase of a reaction initiated at limiting oxygen concentrations relative to substrate, is approximately the same as the 9-HPOD percentage observed during a reaction carried out under low initial oxygen concentration (Fig. 4). During SP, soybean lipoxygenase-1 would catalyze the dioxygenation reaction with a ratio $\approx 50:50$.

Detection of a Free Radical Released from the Enzyme at Low Oxygen Concentration—According to the most widely accepted mechanism (1, 6, 7), presented in the upper part of Scheme 1, it has been hypothesized that the ES' complex could dissociate instead of associating with O_2 , leading to regeneration of the ferrous enzyme (E). Together with this regeneration, a pentadienyl radical (S') would be released in the reaction medium (1, 7). This hypothesis has recently been strengthened by the demonstration that hydrogen abstraction from the substrate at the enzyme catalytic site occurs before molecular oxygen enters the reaction (25). We thus sought the presence of a substrate-based free radical species, released from the enzyme at low oxygen concentration.

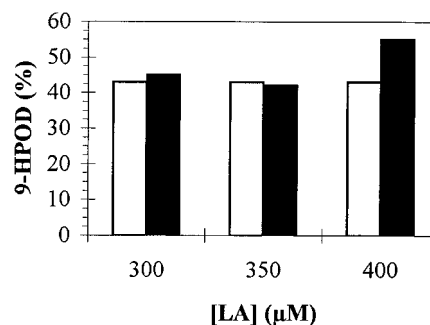


FIG. 5. Observed specificity at low initial oxygen concentration ($< 5 \mu\text{M}$) (■) or calculated specificity during the reaction phase SP of a reaction initiated at $[O_2] = 230 \mu\text{M}$ (□). The calculated $\% 9\text{-HPOD}$ ($(\%9\text{-HPOD})_{\text{SP}}$) is estimated on the basis of the specificity at the end of the reaction as described under "Results."

The production of a free radical under low oxygen concentration has been demonstrated by EPR spectroscopy. The EPR spectrum of $29 \mu\text{M}$ spin label in the presence of linoleic acid in a buffer saturated by bubbling with N_2 for 30 min is shown in Fig. 6A. The reaction was initiated by adding soybean lipoxygenase-1 and carried out under N_2 bubbling. After a 3 min reaction time, the spin label EPR signal has totally disappeared, as shown in Fig. 6B. The EPR signal of the spin label is stable for more than 6 h in the same environment in the absence of enzyme (data not shown). The disappearance of the EPR signal can thus only be attributed to spin label silencing by an enzyme-produced free radical.

This data shows that even at low oxygen concentrations ($< 5 \mu\text{M}$), a radical species is formed by the enzyme. It also shows that during the soybean lipoxygenase-1 reaction, substrate deprotonation occurs before oxygen enters the reaction, in agreement with recently published data (25).

We also used β -carotene bleaching to detect the presence of a free radical dissociated from the enzyme. Soybean lipoxygenase-1 is known to catalyze cooxidation (bleaching) of β -carotene in the presence of linoleic acid (21) resulting in a decrease in β -carotene absorbance at 460 nm. This bleaching is caused by soybean lipoxygenase-1-produced free radicals derived from substrate. To separate the enzyme from β -carotene and thus detect the release of free radical species by the enzyme, the reaction medium containing substrate and enzyme was pumped into a tangential ultrafiltration device. The retentate (enzyme) was recycled into the reaction vessel, and the filtrate (substrate, product, and derived species) was directly flowed into a β -carotene solution circulating as a closed circuit into a spectrophotometer. Thus lipoxygenase is never in contact with the pigment, the bleaching of which can only be ascribed to the presence of free radicals not bound to the enzyme (see "Experimental Procedures"). Under these conditions, Fig. 7 shows that at low oxygen concentrations (N_2 bubbling), the absorbance variation is lower than that caused by β -carotene dilution, indicating the release by the enzyme of free radical species not detectable under higher oxygen concentrations (air bubbling) nor in the absence of enzyme at low oxygen concentrations (data not shown).

Construction and Derivation of the Kinetic Model—According to the current working kinetic scheme proposed by Schilstra *et al.* (1) and presented in the upper part of Scheme 1, soybean lipoxygenase-1 is obtained when purified as a ferrous form (E). This form is catalytically inactive but can bind substrate (S; *e.g.* linoleic acid), thus leading to the observed substrate inhibition. Upon binding a molecule of product (hydroperoxide), this ferrous form is activated to the ferric, catalytically active form (E*). This form is assumed to bind either product (leading to product inhibition) or substrate leading to an E*S complex. The

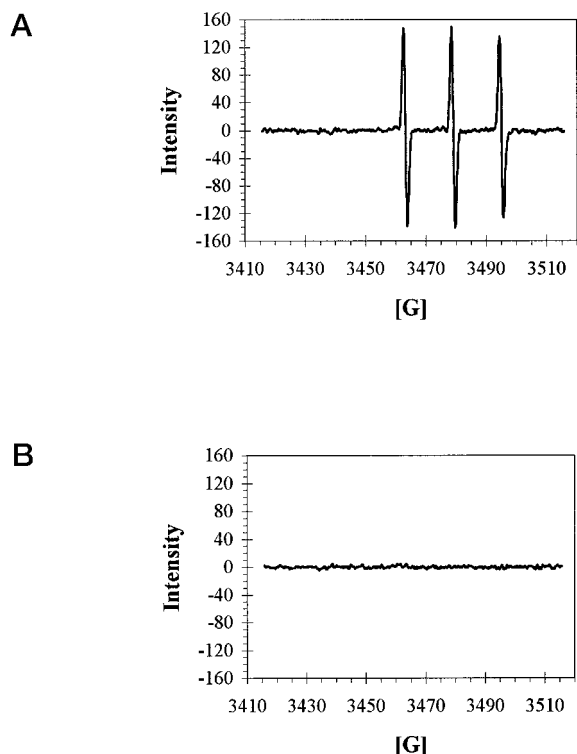


FIG. 6. EPR spectra of 3-(2-bromoacetamido)-PROXYL, 29 μM , in 100 ml of 0.1 M $\text{Na}_4\text{P}_2\text{O}_7$, pH 9.0, buffer containing 625 μM linoleic acid, saturated by bubbling with N_2 for 30 min before the reaction (A) and at 3 min after initiation of the dioxygenation reaction by 20 nM soybean lipoxygenase-1 (B). The buffer was equilibrated by N_2 bubbling throughout the reaction.

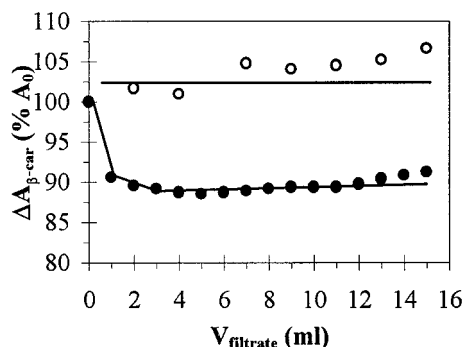


FIG. 7. Absorbance variations during β -carotene cooxidation by the filtrate of a tangential ultrafiltration device separating soybean lipoxygenase-1 (retentate) from free substrate, product and derived species (filtrate) during the course of the dioxygenation reaction (see "Experimental Procedures"). Reaction carried out under N_2 (●) or air (○) bubbling. $[\text{LA}]_{\text{initial}} = 1 \text{ mM}$; $[\beta\text{-carotene}]_{\text{initial}} = 3 \mu\text{M}$; [soybean lipoxygenase-1] = 7.5 nM.

enzyme-catalyzed substrate deprotonation then leads to a complex formed by ferrous enzyme and substrate free radical (probably pentadienyl), ES' . The position of this deprotonation is tightly regulated by the enzyme; with substrates presenting several pentadiene systems (*e.g.* arachidonic acid), one system is preferentially deprotonated depending on the enzyme isoform. The ES' complex then binds O_2 , which is specifically added by the enzyme to either the C-1 or C-5 carbon of the pentadiene system. This regio- (and stereo-) specificity of enzyme-catalyzed O_2 insertion is the basis of the enzyme specificity. In the case of soybean lipoxygenase-1, the specificity observed under nonlimiting oxygen concentrations relative to substrate (13:9 ratio = 95:5), reflects the specificity with which the enzyme catalyzes specifically the insertion of O_2 on the

C-13 carbon. In this case, both the position of substrate deprotonation and O_2 insertion are enzyme controlled. This pathway will thus be referred to as "fully enzymatically" controlled.

To explain the observed change in specificity at low oxygen concentrations, the current working kinetic model was expanded (Scheme 1). This model is based on the model presented by (1) but assumes that the ES' complex can dissociate (as a function of the kinetic constant k_4), leading to the release of a pentadienyl free radical S' in the buffer (Scheme 1, lower part). Our contribution to the model is to hypothesize that this highly reactive radical, once released, could combine with oxygen to form SO_2 . This free radical, as in the classical pentadienyl system auto-oxidation scheme (26, 27), would then associate with either itself leading to termination products (*e.g.* linoleic acid dimers), or with a substrate molecule leading to S' (which contributes to SO_2 regeneration) and a hydroperoxide product, here designated as Q .

During the formation of the hydroperoxide Q , only substrate deprotonation is enzyme controlled but not the O_2 insertion step. Oxygen thus is added in a nonspecific manner, and the 13-HPOD:9-HPOD composition of Q is close to 50:50. This pathway to hydroperoxide production is therefore only "semienzymatically" controlled. P and Q are both linoleic acid hydroperoxides but show different regio-isomeric compositions; they have been artificially differentiated in this scheme only to account for specificity observations. For purposes of simplicity, it has furthermore been considered that $[Q] \ll K_{iP}$, so that product inhibition by Q is not taken into account.

The rates expressing Scheme 1 were derived and simulated to ensure that at high oxygen concentrations the fully enzymatic pathway becomes dominant, leading to marked specificity for 13-HPOD, whereas under low oxygen concentrations, the semienzymatic pathway is preferentially expressed leading to a 13-HPOD:9-HPOD ratio close to 50:50.

Equations 1–10, describing Scheme 1, were obtained with steady-state assumptions, rapid equilibrium assumptions also being made for some segments, and derived as described in Ref. 7.

$$\frac{d[\text{S}]}{dt} = -f_2[X_2] - \left\{ k_6[\text{S}] \sqrt{\frac{k_4}{k_7(k_3[\text{O}_2] + k_4)}} f_2[X_2] \right\} \quad (\text{Eq. 1})$$

$$\frac{d[\text{O}_2]}{dt} = \frac{d[\text{S}]}{dt} \quad (\text{Eq. 2})$$

$$\frac{d[\text{P}]}{dt} = -f_{1P}[X_1] + \left\{ \frac{k_3[\text{O}_2]}{k_3[\text{O}_2] + k_4} f_2[X_2] \right\} \quad (\text{Eq. 3})$$

$$\frac{d[\text{Q}]}{dt} = -f_{1Q}[X_1] + \left\{ k_6[\text{S}] \sqrt{\frac{k_4}{k_7(k_3[\text{O}_2] + k_4)}} f_2[X_2] \right\} \quad (\text{Eq. 4})$$

where

$$f_{1P} = \frac{k_1[\text{P}]}{K_{mP}(1 + ([\text{S}]/K_{iS})) + [\text{P}] + [\text{Q}]} \quad (\text{Eq. 5})$$

$$f_{1Q} = \frac{k_1[\text{Q}]}{K_{mP}(1 + ([\text{S}]/K_{iS})) + [\text{P}] + [\text{Q}]} \quad (\text{Eq. 6})$$

$$f_2 = \frac{k_2[\text{S}]}{K_{mS}(1 + ([\text{P}]/K_{iP})) + [\text{S}]} \quad (\text{Eq. 7})$$

$$[\text{X}_1] = [\text{E}] + [\text{ES}] + [\text{EP}] + [\text{EQ}] \quad (\text{Eq. 8})$$

$$[\text{X}_2] = [\text{E}^*] + [\text{E}^*\text{S}] + [\text{E}^*\text{P}] \quad (\text{Eq. 9})$$

With the steady state approximation, *i.e.*

$$\frac{d[\text{X}_1]}{dt} = \frac{d[\text{X}_2]}{dt} = \frac{d[\text{ES}']}{dt} = 0 \quad (\text{Eq. 10})$$

the system (1–9) simplifies to

$$\frac{d[S]}{dt} = \frac{d[O_2]}{dt} = -(v_O^E + v_O^{SE} + v_{hP} + v_{hQ}) \quad (\text{Eq. 11})$$

$$\frac{d[P]}{dt} = v_O^E - v_{hP} \quad (\text{Eq. 12})$$

$$\frac{d[Q]}{dt} = v_O^{SE} - v_{hQ} \quad (\text{Eq. 13})$$

where

$$v_O^E = \frac{[X_0]}{D} (k_1 k_2 k_3 [S][O_2]([P] + [Q])) \quad (\text{Eq. 14})$$

$$v_O^{SE} = k_6 [S] \sqrt{\frac{[X_0]}{D} \frac{k_1 k_2 k_4 [S]([P] + [Q])}{k_7}} \quad (\text{Eq. 15})$$

$$v_{hP} = \frac{[X_0]}{D} (k_1 k_2 k_4 [P][S]) \quad (\text{Eq. 16})$$

$$v_{hQ} = \frac{[X_0]}{D} (k_1 k_2 k_4 [Q][S]) \quad (\text{Eq. 17})$$

and

$$[X_0] = [X_1] + [X_2] + [ES']$$

$$D = \left\{ k_2 k_4 [S] \left(K_{mP} \left(1 + \frac{[S]}{K_{iS}} \right) + [P] + [Q] \right) \right\} + \left\{ k_1 (k_3 [O_2] + k_4) ([P] + [Q]) \left(K_{mS} \left(1 + \frac{[P]}{K_{iP}} \right) + [S] \right) \right\} + \{ k_1 k_2 [S] ([P] + [Q]) \} \quad (\text{Eq. 18})$$

Equations 14–17 show four different types of rates; two “hydroperoxidase” rates (v_{hP} and v_{hQ}) corresponding to the rate at which P and Q , respectively, are consumed by the enzyme activation, and two dioxygenation rates (v_O^E and v_O^{SE}) corresponding, respectively, to the rate at which the fully enzymatic and semienzymatic reactions occur. Thus v_O^E represents the rate concerning the appearance of P , and v_O^{SE} that concerning the appearance of Q .

To simulate these rates, the kinetic parameters have been estimated. The value of K_{mS} is based on the value of K_M for linoleic acid (see “Experimental Procedures”). The values for k_5 and k_7 are based on those found in the literature for linoleate auto-oxidation (27,28). All other parameters have been estimated as described under “Experimental Procedures” and the corresponding values given in Table III. Except for k_2 and k_6 , the determined values agree well with previously reported results (see Table III). The values for k_2 and k_6 are much higher than those previously reported (1,29,30,31). The significance of these high values is commented on under “Discussion.” The different simulations carried out using the estimated values of Table III fit well to the observed data as shown in Fig.8. As can be seen from Fig.8, *B* and *C*, the fit of the simulation to the observed time-dependent $[O_2]$ variations is slightly worse than to $[HPOD]$ variations. Indeed, the polarographic assay used to follow $[O_2]$ variations is an accurate method to determine relative $[O_2]$ variations (as rate measurement) but is less reproducible when measuring absolute $[O_2]$. This can also be seen from the high standard deviations concerning $[O_2]$ in Fig.8, *B* and *C*. The simulation of $d[P]/dt$ and $d[Q]/dt$ versus $[O_2]_{\text{initial}}$ clearly shows that $d[Q]/dt$ is much less dependent on $[O_2]$ than $d[P]/dt$ (Fig.9). At high $[O_2]$, P appearance is largely predominant, whereas at low $[O_2]$ ($<5 \mu\text{M}$), Q becomes the major product, as a result of the very low P appearance rate.

The 9-HPOD percentage relative to ($[13\text{-HPOD}] +$

TABLE III
Estimated values of the kinetic parameters
for the model shown in Scheme 1

Values determined by other authors are indicated. The numbers in parentheses indicate the reference in which the value is cited. Each parameter has been estimated according to the method described under “Experimental Procedures,” except k_5 and k_7 for which the following values have been used: 5.4×10^8 (28) and 10^7 (27), respectively. The K_{mS} value is based on the estimated value of K_M for linoleic acid (see “Experimental Procedures”).

	Parameter value	Previously determined value (Ref.)
Monomolecular rate constants (s^{-1})		
k_1	250 (± 15)	250 (33); 150 (1); 320 (29)
k_2	$31 (\pm 9) \times 10^3$	350 (31); 300 (1)
k_4	$2.3 (\pm 0.7) \times 10^3$	2.3×10^3 (1)
Bimolecular rate constants ($\text{M}^{-1} \text{s}^{-1}$)		
k_3	$8.0 (\pm 1.7) \times 10^8$	10^9 (1)
k_5	Not estimated	
k_6	$23.5 (\pm 3.5) \times 10^3$	
k_7	Not estimated	
Dissociation constants (μM)		
K_{mS}	40	20 (29); 20 (1)
K_{iS}	$21.7 (\pm 0.8)$	20 (1)
K_{mP}	$20.0 (\pm 0.7)$	16 (33); 20 (1)
K_{iP}	$53 (\pm 9)$	50 (34); 20 (1)

[9-HPOD]) can be simulated with Equations 3 and 4, *i.e.* on the basis of the rates for P and Q formation and their hypothesized regio-isomeric composition (13:9 ratio = 95:5 and 50:50 for P and Q , respectively) with

$$\%9 \text{ HPOD} = \frac{0.5 \times (d[Q]/dt) + 0.05 \times (d[P]/dt)}{(d[Q]/dt) + (d[P]/dt)} \quad (\text{Eq. 19})$$

When calculated according to Equation 19 (Fig. 10), the 9-HPOD percentage tends to be about 6–7% with high ($>200 \mu\text{M}$) oxygen concentrations, whereas the 13-HPOD:9-HPOD ratio tends to be 50:50 at low oxygen concentrations ($\approx 55:45$ at $[O_2] = 5 \mu\text{M}$). The results and simulations presented here are therefore in good agreement with the observed data and the hypothesis presented above.

DISCUSSION

The results presented here show that regiospecificity of soybean lipoxygenase-1 strongly depends upon oxygen concentration. Furthermore, this altered specificity can be expressed during a reaction with “classical” conditions, *i.e.* with a buffer equilibrated with air before the reaction initiation.

These data suggest that when the lipoxygenase reaction is carried out under oxygen concentrations limiting relative to substrate, dioxygenation specificity varies with the reaction course. During the first phase (OC), the initial oxygen concentration is high, and the 13-HPOD:9-HPOD ratio is 95:5. During the second phase (SP), the oxygen concentration is low, and the remaining substrate (not transformed during the first phase) is dioxygenated with a 13-HPOD:9-HPOD ratio $\approx 50:50$.

To account for these experimental findings, we have expanded upon the model presented by Schilstra *et al.* (1), which is based on that proposed by Ludwig *et al.* (7). In this model, the ES' complex can dissociate into E and S' . The occurrence of such a dissociation is highly probable, since we have shown that the enzyme releases substrate-based free radical species under low oxygen concentrations. Our contribution is to specify that the released pentadienyl radical S' can associate with O_2 , leading to formation of a hydroperoxide in a nonspecific manner. The model thus obtained presents two product appearance pathways with different regio-isomeric composition: 13:9 ratio = 95:5 or 50:50. The equations describing the kinetic scheme

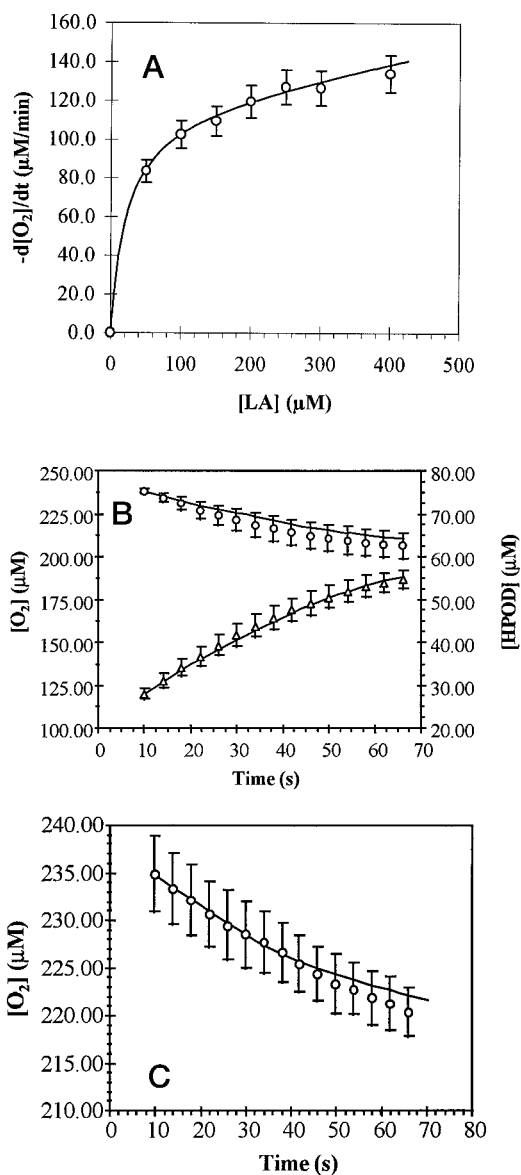


FIG. 8. Comparison of experimental data and simulations carried out using the estimated values of the kinetic parameters shown in Table III. Vertical lines represent standard deviations. A, evolution of the initial rate of oxygen consumption as a function of linoleate concentration for experimental data (\circ) and model simulation (solid line). [soybean lipoxygenase-1] = 9.3 nM; $[O_2]_{\text{initial}} = 230 \mu\text{M}$. B, experimental time-dependent variations in oxygen (\circ) or HPOD (Δ) concentration, and corresponding model simulation (solid line). [soybean lipoxygenase-1] = 7.7 nM, $[O_2]_{\text{initial}} = 245.8 \mu\text{M}$, $[LA]_{\text{initial}} = 43.6 \mu\text{M}$, $[HPOD]_{\text{initial}} = 16.7 \mu\text{M}$. C, experimental time-dependent variations in oxygen concentration (\circ) and respective model simulation (solid line). [soybean lipoxygenase-1] = 7.98 nM, $[O_2]_{\text{initial}} = 236.9 \mu\text{M}$, $[LA]_{\text{initial}} = 22.4 \mu\text{M}$, $[HPOD]_{\text{initial}} = 126.4 \mu\text{M}$. Note that as P and Q (cf. Scheme 1) or 13-HPOD and 9-HPOD cannot be distinguished experimentally when measuring enzyme kinetics, [HPOD] here refers to the total amount of hydroperoxides produced, i.e. $[P] + [Q]$ or $[13\text{-HPOD}] + [9\text{-HPOD}]$.

have been derived and simulations clearly show that the ratio between these two competing pathways, and thus the overall regiospecificity, is dependent upon oxygen concentration.

The values of most of the estimated kinetic parameters are highly correlated with previous studies based on the basic kinetic scheme proposed by Schilstra *et al.* (1), where parameters were estimated with a mathematical treatment similar to that used here (1, 29, 31). One exception nevertheless is the value of the parameter k_2 , which describes the enzyme-cata-

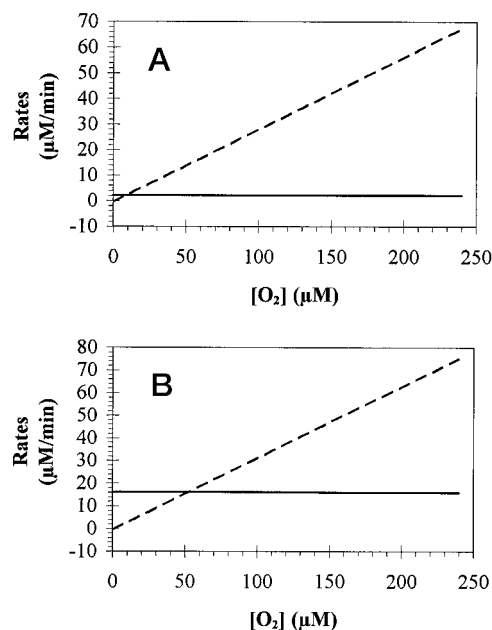


FIG. 9. Simulation of the initial rates $d[P]/dt$ (dotted line) and $d[Q]/dt$ (solid line) as a function of $[O_2]$ with $[LA] = 50 \mu\text{M}$ (A) or $300 \mu\text{M}$ (B). [soybean lipoxygenase-1] = 9.3 nM.

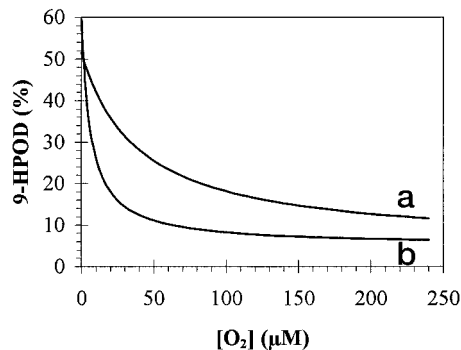


FIG. 10. Simulation of % 9-HPOD as a function of $[O_2]$ with $[LA] = 50 \mu\text{M}$ (a) or $300 \mu\text{M}$ (b). % 9-HPOD is estimated on the basis of the initial rates $d[P]/dt$ and $d[Q]/dt$ as described under "Results." [soybean lipoxygenase-1] = 9.3 nM.

lyzed substrate deprotonation step. This parameter is two orders of magnitude higher than that determined in other studies (29, 31). Furthermore, the bimolecular rate constant k_6 , which expresses the propagation of the semienzymatic pathway (leading to Q) has been estimated in the present study at $23.5 \times 10^3 \text{ M}^{-1} \text{ s}^{-1}$. For the auto-oxidation reaction, the parameter describing the propagation of the free radical, nonenzymatically catalyzed reaction has been reported to be approximately $62 \text{ M}^{-1} \text{ s}^{-1}$ (30), which is 400 times lower than the value determined here. As a result, the k_2 value also increases to account for the rate of Q production. Nevertheless, during auto-oxidation, the reaction is only initiated by linoleate deprotonation, and maintained by the propagation steps. In our model, the semienzymatic way is not only initiated by the k_2 step, but this step also maintains the reaction and provides S' radicals throughout the reaction. The reaction is therefore different from a classical free radical reaction.

Modification of soybean lipoxygenase-1 regiospecificity at low oxygen concentrations has already been reported. In conditions where O_2 concentration is limiting relative to substrate, regiospecificity variations have been demonstrated with rabbit reticulocyte lipoxygenase (7) and presented as a support for the validity of the kinetic model. Our data are consistent with these

observations, but the amplitude of the effect is much larger with soybean lipoxygenase-1; at low oxygen concentrations, the observed 13-HPOD:9-HPOD ratio is approximately 50:50.

Nevertheless, this work is the first to attempt to explain this phenomenon and to incorporate its mechanism into the catalytic scheme of soybean lipoxygenase-1. Moreover, this new completed scheme implies two important characteristics of lipoxygenase catalysis.

First, it implies that, during lipoxygenase catalysis, the lipid substrate is deprotonated before molecular oxygen enters the reaction. Interestingly, this new feature has recently been demonstrated (25).

Furthermore, this model involves a branched mechanism that gives rise to two products that are not distinguishable experimentally when measuring enzyme kinetics. In a recent study (32), it has been considered that such a mechanism would seem unlikely, because the branch in the mechanism would be isotopically insensitive. The overall kinetic isotope effect would result from both pathways (insensitive and sensitive) and thus be lowered. This would be in contrast to the extremely large isotope effect observed during soybean lipoxygenase-1 catalysis (32).

In the model presented here (Scheme 1), the steps described by k_2 and k_3 have been shown to be isotopically sensitive (32), but the step described by k_4 (i.e. the proposed branch) is not isotopically sensitive as it does not involve proton exchange at the enzyme catalytic site. Since the ratio between the steps described by k_3 (leading to *P*) and k_4 (leading to *Q*) is oxygen dependent in our scheme (as shown in Fig. 9), the contribution of the insensitive pathway to the overall isotope effect should be very low at high oxygen concentrations, leading to a strong kinetic isotope effect under these conditions.

With decreasing oxygen concentrations, the ratio between the sensitive and insensitive pathway is modified in favor of the insensitive one so that the latter becomes predominant when $[O_2] < 5 \mu\text{M}$. This model therefore predicts an increase in the kinetic isotope effect with increasing oxygen concentration, which has actually been observed (25, 32). The branched model presented here can therefore explain the magnitude of the observed isotope effect.

Acknowledgments—We thank Dr S. Mottelet (Division Mathématiques Appliquées, Université de Compiègne, France) for precious help concerning the Matlab® program for parameter estimations, and R. Sousa Yeh, professional scientific translator (Paris, France), for criti-

cally reviewing the language of the manuscript. We also are grateful to Prof. M. Le Meste (ENS-BANA, Dijon, France) for the use of the EPR spectrometer and helpful advice on spectra interpretation.

REFERENCES

- Schilstra, M. J., Veldink, G. A. & Vliegthart, J. F. G. (1994) *Biochemistry* **33**, 3974–3979
- Samuelsson, B. (1987) *Science* **237**, 1171–1175
- Schewe, T. (1991) *Trends Biochem. Sci.* **16**, 369–373
- Honn, K. V., Tang, D. G., Gao, X., Butovitch, I. A., Liu, B., Timar, J. & Hagmann, W. (1994) *Cancer Metastasis Rev.* **13**, 365–396
- Gardner, H. W. (1991) *Biochim. Biophys. Acta* **1084**, 221–239
- De Groot, J., Veldink, G., Vliegthart, J. F. G., Boldingh, J., Wever, R. & Van Gelder, B. (1975) *Biochim. Biophys. Acta* **377**, 71–79
- Ludwig, P., Holzhütter, H. G., Colosimo, A., Silvestrini, M. C., Schewe, T. & Rapoport, S. M. (1987) *Eur. J. Biochem.* **61**, 93–100
- Garssen, G. J., Vliegthart, J. F. G. & Boldingh, J. (1971) *Biochem. J.* **122**, 327–332
- Jones, G. D., Russell, L., Darley-Usmar, V. M., Stone, D. & Wilson, M. T. (1996) *Biochemistry* **35**, 7197–7203
- Kühn, H., Schewe, T. & Rapoport, S. M. (1986) *Adv. Enzymol.* **58**, 273–311
- Nikolaev, V., Reddana, P., Whelan, J., Hildenbrandt, G. & Channa Reddy, C. (1990) *Biochem. Biophys. Res. Commun.* **170**, 491–496
- Christopher, J. P., Pistorius, E. K., Regnier, F. E. & Axelrod, B. (1972) *Biochim. Biophys. Acta* **289**, 81–87
- Gardner, H. W. (1989) *Biochim. Biophys. Acta* **1001**, 274–281
- Arai, H., Nagao, A., Terao, J., Suzuki, T. & Takama, K. (1995) *Lipids* **30**, 135–140
- Schnurr, K., Kühn, H., Rapoport, S. M. & Schewe, T. (1995) *Biochim. Biophys. Acta* **1254**, 109–114
- Nelson, M. J., Cowling, R. A. & Seitz, S. P. (1994) *Biochemistry* **33**, 4966–4973
- Pourplanche, C., Lambert, C., Berjot, M., Marx, J., Chopard, C., Alix, A. & Larreta-Garde, V. (1994) *J. Biol. Chem.* **269**, 31585–31591
- Axelrod, B., Cheesbrough, T. M. & Laakso, S. (1981) *Methods Enzymol.* **71**, 441–451
- Galey, J. B., Bombard, S., Chopard, C., Girerd, J. J., Lederer, F., Thang, D.-C., Nam, N. H., Mansuy, D. & Chottard, J. C. (1988) *Biochemistry* **22**, 1058–1066
- Gibian, M. J. & Gallaway, R. A. (1976) *Biochemistry* **15**, 4209–4214
- Zamora, R., Macias, P. & Mesias, J. L. (1988) *Nahrung* **32**, 965–969
- Ramadoss, C. S., Pistorius, E. K. & Axelrod, B. (1978) *Arch. Biochem. Biophys.* **190**, 549–552
- Pourplanche, C., Larreta-Garde, V. & Thomas, D. (1991) *Anal. Biochem.* **198**, 160–164
- Frankel, E. N. (1980) *Prog. Lipid Res.* **19**, 1–22
- Glickman, M. H. & Klinman, J. P. (1996) *Biochemistry* **35**, 12882–12892
- Gardner, H. W. (1989) *Free Radical Biol. Med.* **7**, 65–86
- Roginskii, V. A. (1990) *Mol. Biol.* **24**, 1262–1269
- Schöneich, C., Dilinger, U., Von Bruchhausen, F. & Asmus, K. D. (1992) *Arch. Biochem. Biophys.* **292**, 456–467
- Egmond, M. R., Brunosi, M., Fasella, P. M. (1976) *Eur. J. Biochem.* **61**, 93–100
- Porter, N. A. & Wujek, D. (1984) *J. Am. Chem. Soc.* **106**, 2626–2629
- Schilstra, M. J., Veldink, G. A. & Vliegthart, J. F. G. (1993) *Biochemistry* **32**, 7686–7691
- Glickman, M. H. & Klinman, J. P. (1995) *Biochemistry* **34**, 14077–14092
- Aoshima, H., Kajiwara, T., Hanataka, A., Nakatani, H. & Hiromi, K. (1977) *Biochim. Biophys. Acta* **486**, 121–126
- Wang, Z.-X., Killilea, S. D. & Srivastava, D. K. (1993) *Biochemistry* **32**, 1500–1509